



Nuclear Materials Authority  
P.O.Box 530 Maadi, Cairo, Egypt

ISSN 2314-5609  
Nuclear Sciences Scientific Journal  
7, 87- 100  
2018  
<http://www.ssnma.com>

## RADIOACTIVITY AND ENVIRONMENTAL IMPACTS OF SOME CARBONIFEROUS AND CRETACEOUS KAOLIN DEPOSITS IN SOUTHWESTERN-SINAI, EGYPT

AHMED M. EL-KAMMAR; MOHAMED G. EL-FEKY<sup>1</sup>; HASSAN T. ABU ZIED and  
DINA A. OTHMAN

*Dept. Geology, Fac. Sciences, Cairo Univ., Egypt;<sup>1</sup> Nuclear Material Authority, Kattamiya, Cairo*

### ABSTRACT

Kaolin deposits are among the world's most important and useful industrial materials. In southwestern Sinai, kaolin occurs interbedded with sandstones in east and northeast Abu Zenima area and in southern Cliff of El Tih plateau. The present work is concerned with the natural radioactivity of these kaolin deposits. Naturally occurring radionuclides are measured radiometrically as well as chemically on the representative kaolin samples from Wadi El Iseila, Wadi El Khaboba and Wadi Abansakar. The main target is to discuss the behavior of the naturally occurring radionuclides and to assess their possible environmental hazards and economic importance. The present work characterizes the main radiometric signatures of the Carboniferous and Cretaceous kaolin resources in the studied areas. Calculated environmental parameters indicate that some kaolin types cannot be used as building or decorative material of dwelling.

### INTRODUCTION

Kaolin resources are among the world's most important raw materials for extensive industrial applications. Egypt has large economic reserves of kaolin in many localities, such as in Sinai, Gulf of Suez coast and Kalabsha near Aswan. This paper focuses on the natural radioactivity of kaolin resources of different stratigraphic setting in Sinai. The kaolin deposits of east Abu Zenima area, are mainly interbedded within sandstones of Carboniferous (Weissbrod, 1969) and Cretaceous age (Abu-Zeid, 2008). These deposits have attracted the attention of many geologists for many years; first because of their fairly good quality and ease of accessibility and second because of the assured great reserves in a number of localities (Boulis and Attia, 1994). The kaolin of Wadi El Khaboba that enclosed within the sandstone of Abu Thora Formation has been chosen as

representative of the Lower Carboniferous deposits whereas those in Wadi El Iseila and Wadi Abansakar are enclosed within the Lower Cretaceous Malha Sandstone.

The distribution of the naturally occurring radionuclides mainly uranium ( $^{238}\text{U}$ ), thorium ( $^{232}\text{Th}$ ), potassium ( $^{40}\text{K}$ ) and other radioactive elements, depends on the distribution of rocks from which they originate and the processes which concentrate them. Exposure to ionizing radiation from natural sources is a continuous and unavoidable feature of life on earth. The environmental radiation is composed of the natural radiation, found in the ground, plus the cosmic radiation together with the contribution to the background radiation from nuclear tests and accidents which, eventually, will come down to the ground level. Environmental background radiation varies considerably due to local geological features and at-

mospheric conditions. The radiation dose to the population is from indoor exposure, since people spend most of their time indoors and almost all building materials are radioactive to some degree. The indoor absorbed dose rate varies depending on the type of dwelling, age and the materials used for construction, and location (UNSCEAR, 2000).

**GEOLOGIC SETTING**

The areas under investigation, Wadi El Iseila, Wadi Abansakar and Wadi El Khaboba are located at southwestern Sinai (Fig.1). They are bound by longitudes 33°11' 5" and 33° 15' 00" E and latitudes 29° 04' 30" and 29° 12' 00"N. The studied area at Wadi El Khaboba (Fig. 2) is located between latitudes 29° 04'30" and 29° 05'04" N, and longitudes 33° 13' 20" and 33° 15' 00"E. The Lower Cretaceous sedimentary kaolin of Wadi El Iseila and Wadi Abansakar are belonging to the Malha Formation in north and NE of Abu Zenima and cover an area of 25 km<sup>2</sup> between latitudes 29° 09'51" and 29° 11' 11" N and longitudes 33° 11'52" and 33° 12'56" E (Fig. 3).

Wadi El Iseila and Wadi Abansakar areas are geomorphologically located on a head stream, namely; Wadi El Iseila which is running along the NNE-SSW trend separating Gebel El Iseila to the east and Gebel Abu Edi-



Fig.1: Location map of the studied areas Wadi El-Seila, Wadi Abansakar and Wadi El-Khaboba

emat to the west. At Wadi El Khaboba, the upper clay intercalation of the lower sandy clay member of the Carboniferous Abu Thora Formation consists of two kaolin lenses, which strike N 47° W-S47°E and dip about 20° to NE.

The Carboniferous kaolin deposits in Wadi El Khaboba occur within the Abu Thora Formation (Fig.4), which represents the upper sandstone series of Carboniferous age. Kaolin occurs in the form of two flat, separated lenses with thickness of 2-2.5 m and interbedded within sandstone beds. The kaolin of the lower lens is soft and of grey shades, while that of the upper lens is hard and lighter in color. The harder and lighter colored nature of the upper

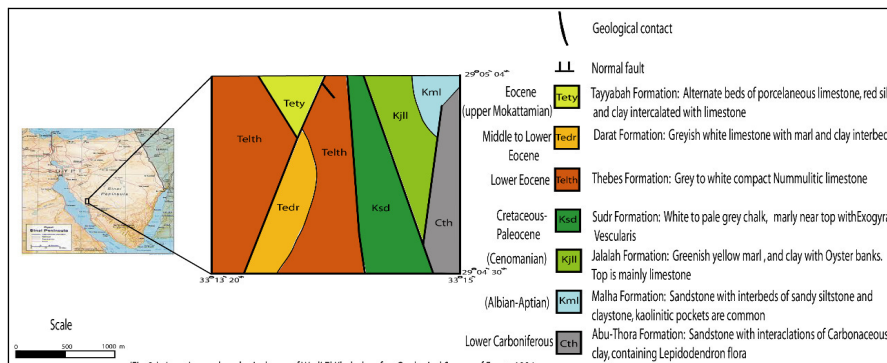


Fig.2: Location and geological maps of Wadi El-Khaboba, (After Geological Survey of Egypt, 1994)

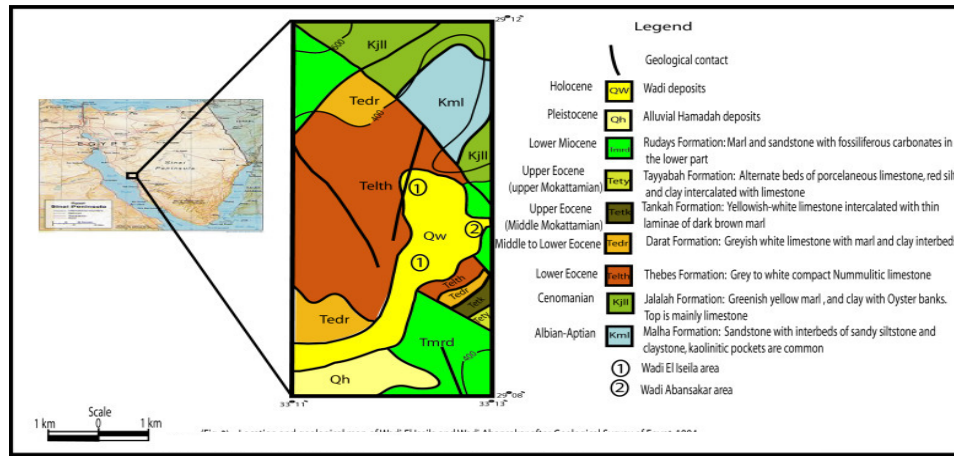


Fig.3: Location and geological maps of El-Iseila and Wadi Abansakar, (After Geological Survey of Egypt, 1994)

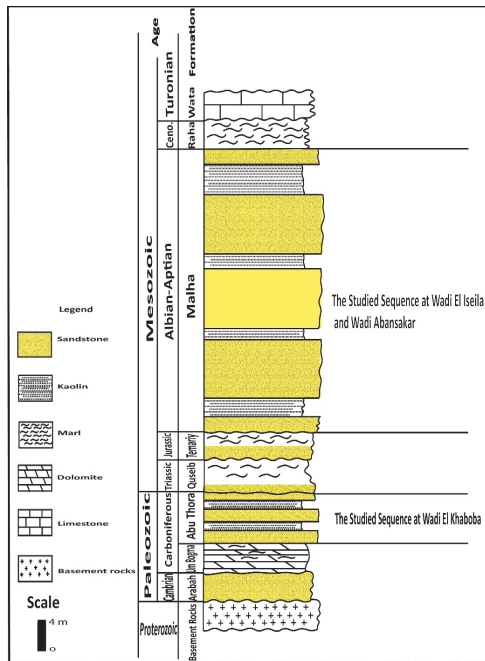


Fig.4: Lithology of Southern Sinai showing the Kaolin bearing formations (Abu Thora & Malha formations), studied areas, (After Geological Survey of Egypt, 1994)

kaolin lens is due to relative enrichment in silt-size quartz fragments (up to 7-10%), with few clusters of very fine sand size. Staining by iron oxy-hydroxides occurs mostly as disseminated spots and enclaves but preferentially concentrate along the bedding planes. The exposed whitish-grey kaolin surfaces, at the upper kaolin lens, are generally polished with development of smooth striation as result of sliding of overlying blocks or presence of shear zone (fault) trending N-15-W and dip 50°.

Kaolin lenses and their hosting sandstone beds are barren of any mega-fossils. Variation in color of kaolin deposit in both lower and upper lenses from grey to red and yellow is controlled by ferrugination, which is best observed particularly in the upper part of the lower lens. The author believes that the coarse-grained porous nature of the sandstone beds of Abu Thora Formation that host the kaolin lenses maintains free infiltration of the ferrugination fluids, where iron oxy-hydroxides precipitate particularly along weak lamination, fractures and bedding planes of the impermeable kaolin. However, the ferrugination in the upper kaolin lens can be observed on a smaller scale as red pigment along bedding plane of

kaolin.

According to Abdallah et al., (1963), the kaolin deposits of Wadi El Iseila and Wadi Abansakar areas interbedded the lower Cretaceous sandstone of Malha Formation (Fig.4). They stated that the basal Malha Formation that hosts the Cretaceous kaolin deposits in Sinai is composed predominantly of grey, ferruginous cross bedded sandstones with few interbeds of green silty shale and calcareous sandstones. Generally, the study lower Cretaceous deposits include higher percentage of quartz fragments, of silt and fine sand-sizes, than the Carboniferous kaolin deposit at Wadi El Khaboba.

### EXPERIMENTAL WORK

The studied kaolin deposits whether of Carboniferous or Cretaceous were examined petrographically and analyzed X-ray diffraction (XRD) analysis to identify the mineral composition in general and the clay mineralogy in particular. The geochemical analysis of the major oxides and trace elements was done by the inductively coupled plasma-mass spectrometry (ICP-MS) in the ACME Lab of Vancouver in Canada. The summary of the descriptive statistics of the chemical analysis data of both Carboniferous and Cretaceous kaolin deposits are quote in Table (1). Twenty three samples were prepared for measuring their contents of U, Th, Ra and K by crushed and ground to about 1mm particle size then kept in a cylindrical plastic container (9.5cm in diameter and 3cm high) which contained about 200ml of the sample. The container was sealed well and left for 28 days to accumulate free radon to attain radioactive equilibrium. The instrument used consists of a bicorn-scintillation detector from NaI (Tl), 76x76mm, with amplifier model NE-4658, and a high voltage power supply model TC-952. Nucleus PCA-8000 computer-based 8192 multichannel analyzer color graphical display Epson LX-80 printer was used. Each sample was measured

twice, 1000 seconds each, and the average of the gross counts was taken. This radiometric analysis was done in the Nuclear Material Authority in Cairo. The obtained data are listed in Table (2).

### MINERALOGICAL AND GEOCHEMICAL CONSIDERATIONS

The X-ray diffraction analysis of oriented, heated and glycolated clay mounts of the studied Carboniferous and Cretaceous kaolin deposits suggests that kaolinite, as a main constituent, is sometimes associated with subsidiary dickite and halloysite, but minor contribution of smectite and illite has also been detected in some samples. The most dominant non-clay mineral is quartz, besides minor gypsum and dolomite, in addition to weak diffractions that can be attributed to hematite. The SEM examination confirms the presence of detrital zircon and monazite in some samples.

In average, the Carboniferous kaolin deposits of Wadi El Khaboba are characterized by higher contents of SiO<sub>2</sub>, MgO, Na<sub>2</sub>O and K<sub>2</sub>O, but lower Al<sub>2</sub>O<sub>3</sub>, TiO<sub>2</sub>, Fe<sub>2</sub>O<sub>3</sub>, CaO and P<sub>2</sub>O<sub>5</sub>, relative to those of the Cretaceous age of Iseila and Abansakar areas (Table 1). Generally, the high Al<sub>2</sub>O<sub>3</sub>/SiO<sub>2</sub> ratio for the Cretaceous kaolin (0.54, in average but up to 0.88) specifies its better grade relative to the Carboniferous kaolin (0.43, in average).

The Carboniferous kaolin is diagnostically enriched in Rb, V and the naturally occurring radionuclides (U and Th). The Th/U ratio increases from 3.05 for the Carboniferous kaolin to 4.07 for the Cretaceous deposits, possibly as a result of relative removal of U from the latter during the pluvial periods. Details on the distribution and equilibrium of the radionuclides are given hereafter. The Carboniferous kaolin deposits are relatively enriched in REE (370 ppm) relative to the Cretaceous ones (288 ppm), however, the PAAS-normalized pattern of the latter show relative preponderance of the HREE over the LREE (Fig. 5).

Table 1: Average, minimum and maximum chemical composition of the studied Carboniferous and Cretaceous kaolin deposits of Sinai

Oxides %, or Elements, ppm	Carboniferous Kaolin			Cretaceous kaolin		
	Mean (n=6)	Minimum	Maximum	Mean (n=14)	Minimum	Maximum
SiO <sub>2</sub>	58.77	57.58	60.62	55.24	44.62	62.45
TiO <sub>2</sub>	1.67	1.39	1.80	2.25	1.19	3.73
Al <sub>2</sub> O <sub>3</sub>	25.51	29.17	22.54	29.30	24.30	39.06
Fe <sub>2</sub> O <sub>3</sub>	1.42	0.61	4.53	2.33	0.60	5.41
MgO	0.37	0.33	0.41	0.07	0.03	0.17
CaO	0.08	0.06	0.11	0.35	0.09	0.55
Na <sub>2</sub> O	0.20	0.14	0.33	0.10	0.01	0.28
K <sub>2</sub> O	0.97	0.74	1.62	0.18	0.04	0.93
P <sub>2</sub> O <sub>5</sub>	0.07	0.06	0.08	0.12	0.05	0.18
L.O.I	10.20	7.49	12.86	10.02	6.43	14.17
Rb	31.5	21	44	1.4	0.2	4.6
Sr	148	112	235	142	30.4	237.6
V	302	124	1080	141	78	206
Co	1.7	0.9	4.3	5.0	2.1	10.3
Ga	41	27	53	41	11	53.4
Zr	547	399	784	671	547	1066
Hf	14	11	20	16	12	26
Nb	74	59	88	87	43	152
Ta	4.6	3.4	5.4	5.4	2.7	9.2
Th	26.3	12	45	17	7	21
U	8.5	6.7	10.6	4.0	2.5	5.7
Y	62	27	119	45	22	61
La	88	49	133	63	11.5	96.6
Ce	158	91	256	124	20	195
Pr	16	10	26	13	2.2	21
Nd	56	38	90	46	7	80
Sm	9.9	5.3	18.2	8.7	2.2	16.7
Eu	1.57	0.85	2.84	1.89	0.56	3.46
Gd	9.6	5.5	17.5	8.2	3.3	14.4
Tb	1.63	0.9	2.98	1.31	0.58	2.12
Dy	11.0	5.2	19.9	8.5	3.9	12.5
Ho	2.22	0.94	4.2	1.64	0.78	2.41
Er	6.45	2.7	12.2	4.9	2.4	6.6
Tm	0.98	0.41	1.76	0.72	0.34	1.0
Yb	6.26	2.82	11.13	4.8	2.4	6.31
Lu	0.93	0.4	1.76	0.73	0.37	0.9
Al <sub>2</sub> O <sub>3</sub> /SiO <sub>2</sub>	0.43	0.37	0.49	0.54	0.39	0.88
Th/U	3.05	1.3	4.6	4.07	2.6	5.4
LREE/HREE	8.66	7.1	10.1	7.9	3.0	11.5
Total REE	370	215	599	288	58	446

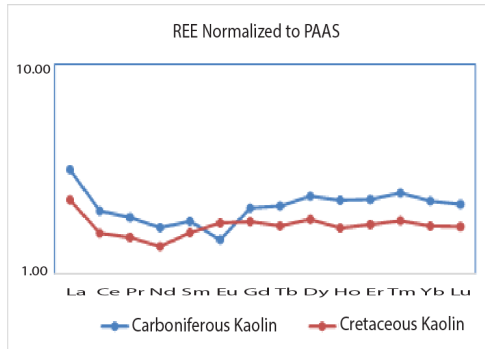


Fig. 5: PAAS-Normalized REE patterns of average Carboniferous and Cretaceous kaolin deposits in the studied areas, Sinai, Egypt

### Distribution of the Radioactive Nuclides

The radiometric measurements were conducted on a total of 21 kaolin samples, representing El Khaboba (7 samples), El Iseila (13 samples), and Abansakar (1 sample). The concentration of eU, eTh, RaeU and K radioactive nuclides, in addition to the calculated eTh/eU, eU/RaeU and Uch/eU ratios in the kaolin samples are listed in Table (2).

It is evident that the Carboniferous kaolin resources of Wadi El Khaboba have higher uranium, thorium, radium equivalent uranium and potassium contents relative to the Cretaceous resources of Wadi El Iseila and Wadi Abansakar. The eU-content in the former ranges between 5 and 18 ppm, averaging 8 ppm, while the content of eTh ranges between 9 and 51 with an average of 29 ppm. Average content of radium equivalent uranium and potassium are 11.4 ppm and 1.9 %, respectively. In contrary, the Cretaceous kaolin of Wadi El Iseila has the lowest eU, eTh, RaeU and K contents where eU ranges between 2 and 8 ppm, averaging 4.9ppm, eTh ranges between 9 and 24 ppm, averaging 18 ppm, Ra (eU) ranges between 6 and 11 ppm, averaging 7.9 ppm and K ranges between 1.15 and 2.24 %, averaging 1.75 % (Table 2).

The average Th/U ratio for Wadi El Khaboba kaolin 3.8 which is quiet similar to those quoted for the Upper Continental Crust by McLennan and Taylor (1980; 1991), and Rudnick and Gao (2004). However, the high Th/U ratio of the studied kaolin could result from a preferential sorption of the “immobile” Th on clay minerals (mostly kaolin), or from a loss of U (as  $UO_2^{2+}$  and/or complexes) relative to Th (De Putter et al., 1999; 2002).

The U-content and Th/U ratio in sedimentary rocks are generally used to deduce the conditions under which the highly anomalous mineralized or uraniferous types were formed (Adams and Weaver, 1958). Therefore, three types of sediments are differentiated according to their Th/U ratio:

i) The first type includes sediments of Th/U ratio ranging between 0.012 and 0.81. These sediments are developed under conditions where uranium was removed from its source and fixed in the sediments with continuous recharge.

ii) The second type of sediments has Th/U ratio varying between 1.47 and 1.49. They are characterized by their relatively high Th-content due to slightly more scavenging of U-content because of continuous leaching and recharging.

iii) The third type of sediments, exhibits Th/U ratio ranging between 1.49 and 5.47. These sediments reflect the poor weathering and rapid deposition of rock detritus. This type is dominant in detrital radioactive minerals such as xenotime, samarskite, thorite and euxenite usually dominate them.

The obtained data indicate that the eTh/eU ratio of Wadi El Khaboba, Wadi El Iseila and Wadi Abansakar are high and related to the third group reflecting their relatively low uranium content in some samples. The eU-eTh variation diagram (Fig.6) confirms these results where most of the samples fall in the field of  $eTh/eU \geq 2$ .

Table 2 : Concentration of radionuclides and their ratios for the studied kaolin resources of Wadi El Khaboba, Wadi El Iseila and Wadi Abansakar.

Sample	Location	Sample	eU	eTh	Ra	K	eTh/e	eU/Rae	U <sub>c</sub>	U <sub>e</sub> /e
Sandy	Wadi el	51	3	20	7	1.8	6.67	0.43	4.00	1.33
Pebbly	Wadi el	21	UL	9	8	1.8			2.80	
Ferrugina	Wadi el	54	6	22	9	1.1	3.67	0.67	4.60	0.77
Ferrugina	Wadi el	33	5	24	11	1.9	4.80	0.45	5.70	1.14
Silty	Wadi el	22,26	2	23	7	2.2	11.50	0.29	5.00	2.50
Grey	Wadi el	35,32	UL	23	6	1.8			3.50	
Sandy	Wadi el	31	8	12	8	1.8	1.50	1.00	3.40	0.43
Sandy	Wadi el	42	7	15	7	1.7	2.14	1.00	3.90	0.56
Silty	Wadi el	22	UL	14	10	1.5			5.00	
Sandy	Wadi el	45	UL	18	7	1.5			3.90	
Sandy	Wadi el	31	2	15	7	1.2	7.50	0.29	3.40	1.70
Sandy	Wadi El	41	7	19	9	1.5	2.71	0.78	4.20	0.60
Ferrugina	Wadi El	43	4	19	8	2	4.75	0.50	3.60	0.90
Ferrugina	Wadi El	23	UL	23	7	2.1			3.90	
av			4.89	18.2	7.93	1.7	5.03	0.60	4.06	1.10
Min.			2.00	9.00	6.00	1.1	1.50	0.29	2.80	0.43
Max.			8.00	24.0	11.0	2.2	11.5	1.00	5.70	2.50
Silty	Wadi El	5	8	51	10	2.6	6.38	0.80	8.20	1.03
Silty	Wadi El	8	5	28	12	2.2	5.60	0.42	8.20	1.64
Silty	Wadi El	9	6	30	13	2.6	5.00	0.46	8.20	1.37
Silty	Wadi El	6	15	51	12	1.5	3.40	1.25	10.6	0.71
Silty	Wadi El	7	11	33	15	2.5	3.00	0.73	8.30	0.75
Grey	Wadi El	2	8	13	10	1.1	1.63	0.80	6.80	0.85
Ferrugina	Wadi El	3	5	18	7	0.8	3.60	0.71	6.70	1.34
Grey	Wadi El	4	5	9	12	1.3	1.80	0.42	10.5	2.10
av			7.88	29.1	11.3	1.8	3.80	0.70	8.44	1.22
			8.00	9.00	7.00	0.8	1.63	0.42	6.70	0.71
Max.			15.0	51.0	15.0	2.6	6.38	1.25	10.6	2.10
Grey	WadiAbansa	62	UL	23	9	2.4			5.40	
Min.			2.00	9.00	6.00	0.8	1.50	0.29	2.80	1.21
Max.			15.0	51.0	15.0	2.6	11.50	1.25	10.6	0.43
Av.			6.29	22.2	9.17	1.8	4.45	0.65	5.64	2.50

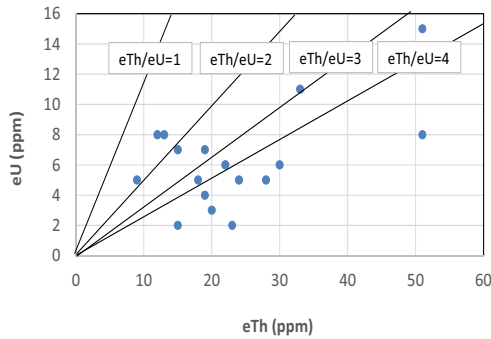


Fig. 6 : The eU versus eTh of the studied kaolin deposits of Sinai

### Radioactive Equilibrium/Disequilibrium

The study of radioactive equilibrium/ disequilibrium is considered an essential part of the radiometric investigations of uranium ore deposits and U-bearing rocks. It sheds some lights on the surface weathering, alteration and movement of uranium by groundwater. It also helps to explain the isotopic variation of some radioactive nuclides and consequently can be used as a tool for U-exploration processes. The equilibrium state means a closed system (for physical and chemical exchanges of the radionuclides) with the surrounding environments whereas disequilibrium indicates an open system, i.e., the radioactive nuclides may migrate out from their parents. The liberated radionuclides can be accumulated through several chemical and geological processes, including; chemical weathering, precipitation of minerals from aqueous solutions by biological and inorganic processes, adsorption on suspended clay minerals, etc.

In recent years, the radioactive equilibrium/ disequilibrium study has been applied on different geological processes during Quaternary such as sedimentation in marine and continental environments (Burnett and Veeh, 1992), soil formation and evolution (Mathieu et al., 1995), and in dating sedimentary and volcanic rocks younger than 300,000 years (Ivanovich

et al., 1992). There are several methods and ways by which the evidences and parameters of radioactive equilibrium /disequilibrium states are estimated. These include:

i) Measurement of uranium content in the rocks or ores using chemical techniques, where uranium is expressed as (Uc) as well as radiometric analysis, where uranium is expressed as Ur. The equilibrium ratio (ER) is given as  $ER = U_c/U_r$  (Hansink, 1976). The equilibrium is attained if  $ER = 1$ , otherwise disequilibrium is predominant.

ii) Measurement of both the equivalent uranium (eU) and radium (RaeU) concentrations (in ppm) radiometrically. The equilibrium factor (P) is given as  $P = eU/RaeU$  (El Galy et al., 2008).

iii) Measurement of the activity ratios (ARs) between the parent U-238 and/or Th-232 nuclides and their/its daughters, especially those of long half-lives, such as  $^{238}\text{U}/^{226}\text{Ra}$ ,  $^{226}\text{Ra}/^{214}\text{Pb}$ ,  $^{214}\text{Pb}/^{214}\text{Bi}$ ,  $^{214}\text{Pb}/^{238}\text{U}$ ,  $^{228}\text{Ra}/^{232}\text{Th}$  (Cochran, 1992). The equilibrium is achieved if the activity ratio between the parent/daughter or between daughter/daughter is equal to unity.

In the present study, the radioactive equilibrium/ disequilibrium states of the investigated kaolin deposits are discussed through the equilibrium factor (P), i.e.  $P = eU/RaeU$ , and ER, i.e.  $ER = U_c/U_r$ . The obtained results indicate that in the equilibrium factor in most samples is less than unity (Fig. 7). This reflects a state of radioactive disequilibrium due to leaching of eU relative to RaeU. This is also the case of ER factor in Wadi El Khaboba kaolin. On the other hand, the ER factor of Wadi El Iseila kaolin is higher than unity suggesting disequilibrium as a result of uranium enrichment. This is probably attributed to recent addition of U during the pluvial periods. It could be concluded that the latest enrichment of U in the studied sediments took place within the last 1.5 Ma as there was no enough time to restore equilibrium.

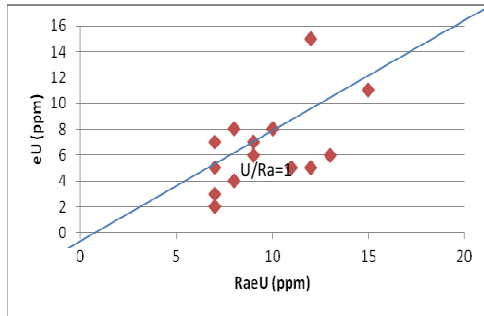


Fig. 7: eU versus Ra of the studied kaolin deposits of Sinai

**Activity Concentrations**

Activity concentrations of <sup>238</sup>U, <sup>232</sup>Th, <sup>226</sup>Ra and <sup>40</sup>K were measured in the studied kaolin samples. The <sup>238</sup>U activity concentration ranges between 0.0 and 186, averaging 57.7 Bqkg<sup>-1</sup>, <sup>232</sup>Th varies between 36 and 206Bqkg<sup>-1</sup> (av. 90 Bqkg<sup>-1</sup>). <sup>40</sup>K ranges between 266 and 820 Bqkg<sup>-1</sup> with average 571 Bqkg<sup>-1</sup>. The world concentration limits of <sup>238</sup>U, <sup>232</sup>Th and <sup>40</sup>K are equal to 35, 30 and 400 Bqkg<sup>-1</sup> respectively (UNSCEAR, 2000). The studied kaolin samples have much higher activity values relative to that recorded by the UNSCEAR (2000).

**Hazard Indices**

**Absorbed dose rate in air (D)**

According to Ğ ğn et al. (2007), the absorbed gamma dose rates in air, at 1m above the ground surface, for the uniform distribution of radionuclides (<sup>238</sup>U, <sup>232</sup>Th and <sup>40</sup>K) were calculated on the basis of guide lines provided by UNSCEAR (2000) by the following Eq. (1)

$$D \text{ (nGy h}^{-1}\text{)} = 0.462A_U + 0.604A_{Th} + 0.0417A_K \quad (1)$$

The values of eU, eTh and RaeU, in ppm, as well as K, in %, were converted to activity concentration, Bq kg<sup>-1</sup>, using the conversion factors given by the Polish Central Laboratory

for Radiological Protection (Malczewski et al., 2004).

Where; A<sub>U</sub>, A<sub>Th</sub> and A<sub>K</sub> are the average specific activities of <sup>238</sup>U, <sup>232</sup>Th and <sup>40</sup>K in Bq/kg, respectively.

The estimated indoor gamma dose rate values for the kaolin samples are given in Table 3. The DR values for Wadi El Iseila kaolin samples range from 46 to 113 nGy h<sup>-1</sup> with a mean value of 856 nGy h<sup>-1</sup>. For Wadi El Khaboba, the DR ranges from 69 to 230 nGy h<sup>-1</sup> with a mean value of 141 nGy h<sup>-1</sup>. The mean DR values for WadiEl Iseila and Wadi El Khaboba kaolin samples exceed the world average value of soils (55 nGy h<sup>-1</sup>, Yang et al., 2005).

**Annual effective dose equivalent (AEDE)**

The annual effective dose equivalent (AEDE) was calculated from the absorbed dose by applying the dose conversion factor of 0.7 Sv/Gy and the outdoor occupancy factor of 0.2 (UNSCEAR, 2000, Ğ ğn et al., 2007). Furthermore, the average values of the annual effective dose for all kaolin samples are also listed in Table (3). The mean values of Wadi El Iseila and Wadi El Khaboba kaolin samples are 0.10 and 0.17, which are less than 0.48 mSvy<sup>-1</sup> recommended by UNSCEAR (2000) as a worldwide average of the annual effective dose.

**Radium equivalent activity (Ra<sub>eq</sub>)**

The radium equivalent activity for the samples was calculated. According to Tufail,et al., (1992), the exposure to radiation can be defined in terms of the radium equivalent activity (Ra<sub>eq</sub>), which can be expressed by the following equation:

$$Ra_{eq} = A_U + 10/7A_{Th} + 10/130A_K \quad (2)$$

where, A<sub>U</sub>, A<sub>Th</sub> and A<sub>K</sub> are the specific activities of U, Th and K, respectively, in Bq/kg.

The range and the mean values of Ra<sub>eq</sub> of kaolin samples are presented in Table 3. The

Table 3: The estimated indoor gamma dose rate values, average values of annual effective dose as well as the range and the mean value of  $R_{aeq}$  of the studied kaolin resources

Sample	Location	eU	eTh	Ra	K	Abs.	Eff.	$R_{aeq}$	$H_{ex}$	$H_{in}$	$I_{\gamma}$
Sandy	Wadi el Iseila	37.2	80.8	77.7	582.18	90.27	0.11	237.91	0.53	0.63	1.44
Pebbly	Wadi el Iseila	0	36.36	88.8	582.18	46.24	0.06	185.53	0.26	0.26	0.75
kaolin											
Ferrugina	Wadi el Iseila	74.4	88.88	99.9	359.95	103.07	0.13	254.56	0.62	0.82	1.62
ted kaolin											
Ferrugina	Wadi el Iseila	62	96.96	122.1	616.61	112.92	0.14	308.05	0.67	0.84	1.79
ted kaolin											
Silty	Wadi el Iseila	24.8	92.92	77.7	701.12	96.82	0.12	264.38	0.57	0.64	1.56
Grey	Wadi el Iseila	0	92.92	66.6	563.4	79.62	0.10	242.68	0.48	0.48	1.30
Sandy	Wadi el Iseila	99.2	48.48	88.8	566.53	98.74	0.12	201.64	0.57	0.84	1.52
Sandy	Wadi el Iseila	86.8	60.6	77.7	550.88	99.68	0.12	206.65	0.58	0.82	1.55
Silty	Wadi el Iseila	0	56.56	111	491.41	54.65	0.07	229.60	0.32	0.32	0.89
Sandy	Wadi el Iseila	0	72.72	77.7	491.41	64.41	0.08	219.39	0.38	0.38	1.05
Sandy	Wadi el Iseila	24.8	60.6	77.7	391.25	64.38	0.08	194.37	0.38	0.45	1.03
Sandy	Wadi El Iseila	86.8	76.76	99.9	485.15	106.70	0.13	246.88	0.63	0.87	1.67
Ferrugina	Wadi El Iseila	49.6	76.76	88.8	626	95.38	0.12	246.61	0.56	0.69	1.52
ted kaolin											
Ferrugina	Wadi El Iseila	0	92.92	77.7	660.43	83.66	0.10	261.25	0.50	0.50	1.37
ted kaolin											
av		38.9	73.87	88.01	547.75	85.47	0.10	235.68	0.50	0.61	1.36
Min.		0.00	36.36	66.60	359.95	46.24	0.06	185.53	0.26	0.26	0.75
Max.		99.2	96.96	122.1	701.12	112.92	0.14	308.05	0.67	0.87	1.79
Silty	Wadi El	99.2	206.0	111	820.06	204.48	0.25	468.42	1.23	1.50	3.27
Silty	Wadi El	62	113.1	133.2	704.25	126.34	0.15	348.97	0.75	0.92	2.01
Silty	Wadi El	74.4	121.2	144.3	816.93	141.64	0.17	380.28	0.84	1.04	2.25
Silty	Wadi El	186	206.0	133.2	475.76	230.22	0.28	464.14	1.40	1.90	3.62
Silty	Wadi El	136.	133.3	166.5	804.41	177.09	0.22	418.83	1.05	1.42	2.78
Grey	Wadi El	99.2	52.52	111	363.08	92.69	0.11	213.96	0.55	0.81	1.43
Ferrugina	Wadi El	62	72.72	77.7	266.05	83.66	0.10	202.05	0.50	0.67	1.32
Grey	Wadi El	62	36.36	133.2	435.07	68.75	0.08	218.61	0.40	0.57	1.07
av		97.6	117.6	126.2	585.70	140.61	0.17	339.41	0.84	1.10	2.22
Min.		62.0	36.36	77.70	66.05	68.75	0.08	202.05	0.40	0.57	1.07
Max.		186.	206.0	166.5	820.06	230.22	0.28	468.42	1.40	1.90	3.62
Grey	WadiAbansak	0	92.92	99.9	779.37	88.62	0.11	292.59	0.52	0.52	1.45
Min.		0.00	36.36	66.60	266.05	46.24	0.06	185.53	0.26	0.26	0.75
Max.		186.	206.0	166.5	820.06	230.22	0.28	468.42	1.40	1.90	3.62
Av.		57.6	89.93	101.8	571.02	104.78	0.13	274.23	0.62	0.78	1.66
International average		35	30	-	400	55	0.48	370	1	1	0.5

mean  $Ra_{eq}$  values for Wadi El Iseila and Wadi El Khaboba samples (236 Bq kg<sup>-1</sup> and 339 Bq kg<sup>-1</sup>, respectively) are below the criterion limit of 370 Bq kg<sup>-1</sup>, except for some samples from Wadi El Khaboba (Table 3).

**External and internal hazard index ( $H_{ex}$  and  $H_{in}$ )**

To limit the annual external gamma-ray dose (Saito and Jacob, 1995; Saito et al., 1998; UNSCEAR, 2000) to 1.5 Gy for the samples under investigation, the external hazard index ( $H_{ex}$ ) is given by the following equation:

$$H_{ex} = A_U/370 + A_{Th}/259 + A_K/4810 \quad (3)$$

The internal exposure to <sup>222</sup>Rn and its radioactive progeny is controlled by the internal hazard index ( $H_{in}$ ), which is given by Nada (2003):

$$H_{in} = A_U/185 + A_{Th}/259 + A_K/4810 \quad (4)$$

These indices must be less than unity in order to keep the radiation hazard insignificant (Lakehal, et al., 2010 and Baykara et al., 2010).

The value of this index must be less than unity for the radiation hazard to be negligible, i.e. the radiation exposure due to radioactivity in construction materials must be limited to 1.5 mSv y<sup>-1</sup>. The values of the external hazard ( $H_{ex}$ ) for the studied kaolin of Wadi El Isila are less than unity which agrees with the recommended values. In contrast, the values of the internal hazard indices ( $H_{in}$ ) for Wadi El Khaboba samples are higher than unity indicating their kaolin cannot be used as building or decorative material of dwelling.

**Activity concentration index ( $I\gamma$ )**

Another radiation hazard index, known as the representative level index,  $I\gamma$  (NEA-OECD, 1979) is defined as follows:

$$I\gamma = A_U/150 + A_{Th}/100 + A_K/1500 \quad (5)$$

Where,  $A_U$ ,  $A_{Th}$  and  $A_K$  are the activity concen-

trations of <sup>238</sup>U, <sup>232</sup>Th and <sup>40</sup>K, respectively in Bq/kg (Abbady, et al., 2005). The safety value for this index is ≤ 1 (El Galy, et al., 2008; El Aassy, et al., 2012).

Table 3 shows the mean values of the gamma-index ( $I\gamma$ ) kaolin samples are 1.36 and 2.22 for Wadi El Iseila and Wadi El Khaboba, respectively, which are higher dose criterion (0.3 mSv/y) and correspond to an activity concentration index of 2 ≤  $I\gamma$  ≤ 6 proposed by EC (1999) for materials used in bulk construction.

Contribution of <sup>238</sup>U, <sup>232</sup>Th and <sup>40</sup>K radionuclides for the absorbed dose rate within the studied rocks are plotted on Fig.(8). It is evident that <sup>40</sup>K plays the main and most important role in the dose rate contribution.

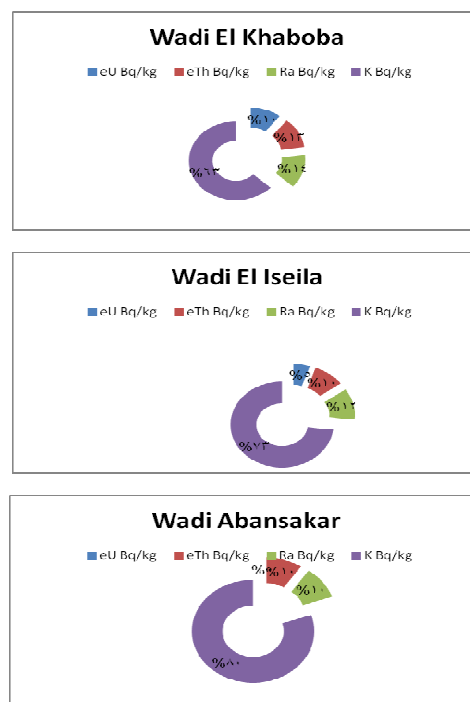


Fig 8 : Contribution of <sup>238</sup>U, <sup>232</sup>Th and <sup>40</sup>K radionuclides for the absorbed dose rate within the studied rock samples

### CONCLUDING REMARKS

The study of the radioactivity of the Carboniferous (Wadi El Khaboba) and Cretaceous (Wadi El Iseila and Wadi Abansakar) kaolin deposits reveals that the Carboniferous kaolin of have higher uranium, thorium, radium and potassium contents relative to the Cretaceous deposits. The obtained data indicate that the eTh/eU ratio of Sinai kaolin is generally high and follows the third group of low uranium possibly as a result of weathering and rapid deposition of rock detritus. In most samples, the equilibrium factor is less than unity. This reflects a state of radioactive disequilibrium due to leaching of eU relative to Ra. This is also the case of ER factor in Wadi El Khaboba kaolin. On the other hand, the ER factor of Wadi El Iseila kaolin is higher than unity suggesting disequilibrium as a result of secondary uranium uptake. This can principally be attributed to recent addition of U during the pluvial periods. It could be concluded that the latest enrichment of U in the studied sediments had taken place within the last 1.5 m.y. as there was not enough time to restore equilibrium. The studied kaolin samples have much higher activity values relative to that recorded by the *UNSCEAR (2000)*. Accordingly, it is no recommended to use the Carboniferous kaolin deposits in the industrial purposes due to their radioactive enrichment.

### REFERENCES

- Abdallah, A.M.; Adindani, A., and Fahmy, N., 1963. Stratigraphy of Upper Paleozoic Rocks, Western Side of the Gulf of Suez, Egypt. *Egyptian Geol. Surv.*, 18 p.
- Abu-Zeid, R.H., 2008. Lithostratigraphy and biostratigraphy of some Lower Cretaceous outcrops from Northern Sinai, Egypt. *Cretaceous Research*, 29, 603-624.
- Adams, J.A.S., and Weaver, C.E., 1958. Thorium to Uranium Ratios as Indicator for Sedimentary Processes; an Example of Geochemical Facies. *Am. Assoc. Pet. Geol. Bull.*, 42, 397-430.
- Baykara, O.; Karatepe, S., and Dođru, M., 2011. Assessments of natural radioactivity and radiological hazards in construction materials used in Elazığ, Turkey. Technical Report. *Radiation Measurements*, 46, 153-158.
- Boulis, S.N., and Attia, A.K.M., 1994. Mineralogical and chemical composition of Carboniferous and Cretaceous kaolins from a number of localities in Egypt. *e Mineral. Soc. Egypt*, 100p.
- Burnett, W.C., and Veeh, H.H., 1992. Uranium-series studies of marine phosphates and carbonates. In: *Uranium-series Disequilibrium: Applications to Earth, Marine and Environmental Sciences* (Ivanovich, M. And Harmon, R.S., Eds). 2<sup>nd</sup> Ed., Science Publications, Oxford Univ. Press, Oxford, 487-512.
- Cochran, J.I K., 1992. The oceanic chemistry of the uranium-and thorium-series nuclides. In: *Uranium-series Disequilibrium: Applications to Earth, Marine and Environmental Sciences* (Ivanovich, M. And Harmon, R.S., Eds). Clarendon Press, Oxford, p. 334-395.
- De Putter, Th.; Bernard, A.; Perruchot, A.; Yans, J.; Verbrugge, Fr., and Dupuis, Chr., 2002. Neoformed mineral parageneses in acid weathering systems: sedimentary vs volcanic environments. *Proc. 12<sup>th</sup> Inter. Clay Conf.*, Elsevier Oxford.
- De Putter, Th.; Charlet, J.-M., and Quinif, Y., 1999. REE, Y and U concentration at the fluid-iron oxide interface in Late Cenozoic cryptodolines from Southern Belgium. *Chem. Geol.*, 153, 139-150.
- El-Aassy I. E.; Afaf A. ;Nada, El-Galy, M.M.; El-Feky M.G.; Abdel Maksoud, T.M.; Talaat, Sh.M., and Ibrahim, E.M., 2012. Behavior and environmental impacts of radionuclides during the hydrometallurgy of calcareous and argillaceous rocks, Southwestern Sinai, Egypt. *Applied Radiation and Isotopes*, 70, 1024-1033.
- European Commission (EC) , 1999. Radiation protection 112 – radiological protection principles concerning the natural radioactivity of building materials. Directorate- General Environment, Nuclear Safety and Civil Protection.

- El Galy, M.M.; El Mezayn, A.M.; Said, A.F.; El Mowafy, A.A., and Mohamed, M.S., 2008. Distribution and environmental impacts of some radionuclides in sedimentary rocks at Wadi Nasseib area, southwest Sinai, Egypt. *J. Environ. Radioact.*, 99, 1075–1082.
- Hansink, J. D. , 1976. Equilibrium analysis of sandstone roll-front uranium deposits. *Proceeding of International Symposium on Exploration of uranium ore deposits.* IAEA, Vienna, 683-693.
- Ivanovich, M., and Latham, A. G., Ku, L., 1992. Uranium series disequilibrium applications in geochronology. In: *Uranium series disequilibrium: Applications to Earth, marine and environmental sciences* (Ivanovich, M., and Harmon, R. S., Eds.). 2<sup>nd</sup> Ed. Science Publications, Oxford Univ. Press, Oxford, 62-85.
- Lakehal, Ch.; Ramdhane, M., and Boucenna, A., 2010. Natural radionuclide concentrations in two phosphate ores of East Algeria. *J. Environ. Radioact.*, 101, 377–379.
- Malczewski S.; Teper L., and Dorda J., 2004. Assessment of natural and anthropogenic radioactivity levels in rocks and soils in the environs of ŚwieradówZdrój in Sudetes, Poland, by in situ gamma-ray spectrometry”, *J. Environmental Radioactivity* , 73, 233–245.
- Mathieu, D.; Bernat, M., and Nahon, D., 1995. Short-lived U and Th isotope distribution in a tropical laterite derived from granite (Pitinga river basin, Amazonia, Brazil): application to assessment of weathering rate. *Earth Planet. Sci. Lett.*, 136, 703-714.
- McLennan, S.M., and Taylor, S.R., 1980. Rare earth element–thorium correlations in sedimentary rocks and the composition of the continental crust. *Geochimica et Cosmochimica Acta*, 44, 1833–1839.
- McLennan, S.M., and Taylor, S.R., 1991. Sedimentary rocks and crustal evolution: tectonic setting and secular trends. *J. Geol.*, 99, 1–21.
- Nada, A., 2003. Evaluation of natural radionuclides at Um-Greifat area, Eastern Desert of Egypt. *Appl. Radiat. Isot.* ,58, 275–280.
- NEA-OECD, Nuclear Energy Agency., 1979. Exposure to Radiation from Natural Radioactivity in Building Materials. Report by NEA Group of Experts. OECD, Paris.
- Özün, Y.; Altınsoy N., S; Ahin, S.Y.; Güngör, Y.; Gültekin, A.H.; Karahan, G., and Karacık, Z., 2007. Natural and anthropogenic radionuclides in rocks and beach sands from Ezine region (Canakkale), Western Anatolia, Turkey. *Appl. Radiat. Isot.* ,65 ,739–747
- Rudnick, R.L., and Gao, S., 2004. Composition of the Continental Crust. In: *Treatise on Geochemistry* ( Holland, H.D. and Turekian, K.K. ,Eds.). Elsevier, Amsterdam, 3, 1-64.
- Saito, K., and Jacob, P., 1995. Gamma ray fields in the air due to sources in the ground. *Radiat. Prot. Dosim.* ,58, 29-45.
- Saito, K.; Petoussi, H., and Zanki, M., 1998. Calculation of the effective dose and its variation from environmental gamma ray sources. *Health Phys.*, 74, 698–706.
- Tufail, M.; Ahmad, N.; Mirza, S.M.; Mirza, N.M., and Khan, H.A., 1992. Regular paper, natural radioactivity from the building materials used in Islamabad and Rawalpindi, Pakistan. *Sci. Total Environ.*, 121, 283–291.
- United Nations Scientific Committee on Effects of Ionizing Radiations ,UNSCEAR., 2000. United Nations Scientific Committee on the effects of atomic radiation, sources and effects of ionizing radiation. Report to General Assembly, with Scientific Annexes United Nations. United Nations, New York
- Weissbrod, T., 1969. The Paleozoic of Israel and adjacent countries, part II: The Paleozoic outcrops in Southwestern Sinai and their correlation with those of southern Israel. *Israel Geol. Surv. Bull.*, 48, 32 p.
- Yang, Y.; Wu, X.; Jiang, Z.; Wang, W.; Lu, J.; Lin, J.; Wang, L., and Hsia, Y., 2005. Radioactivity concentration in soils of the Xiazhuang granite area, China. *Appl. Radiat. Isot.*, 63, 255–259.

## النشاط الإشعاعي و الأثر البيئي لبعض رواسب الكاولين من العصر الكربوني و العصر الطباشيري في جنوب غرب سيناء بمصر

أحمد محمد الكمار ، محمد جلال الفقى ، حسن طه ابو زيد و دينا احمد عثمان

رواسب الكاولين من اهم الخامات الصناعية. فى جنوب غرب سيناء, يتواجد الكاولين على هيئة عدسات متعاقبة مع الحجر الرملى فى شرق و شمال شرق منطقة ابو زنيمة و فى الجرف الجنوبي لهضبة التيه (جنوب وسط سيناء). العمل الحالى يهتم بدراسة النشاط الاشعاعى الطبيعى لرواسب الكاولين. تم قياس النويدات المشعه الموجودة طبيعيا, اشعاعيا و كذلك كيميائيا على عينات تمثيلية من الكاولين تم جمعها من وادى العسيله, وادى الخبويه و وادى ابنسك. الهدف الرئيسى هو مناقشة سلوك النويدات المشعه طبيعيا و تقييم مخاطرها البيئية المحتملة و الاهميه الاقتصادية. العمل الحالى يوصف البصمة الاشعاعية الرئيسية لموارد رواسب الكاولين فى اماكن الدراسة. المعايير البيئية المحسوبة تشير الى ان بعض انواع الكاولين لا يمكن ان تستخدم فى مواد البناء او كمواد ديكور فى المسكن.